Extended ultrahigh-Q-cavity diode laser

Zhenda Xie,[1,2] Wei Liang,[3] Anatoliy A. Savchenkov,[3] Jinkang Lim,[1] Jan Burkhart,[2] Mickey McDonald,[4] Tanya Zelevinsky,[4] Vladimir S. Ilchenko,[3] Andrey B. Matsko,[3] Lute Maleki,[3] and Chee Wei Wong[1,2,*]

[1]*Mesoscopic Optics and Quantum Electronics Laboratory, University of California, Los Angeles, California 90095, USA*

[2]*Optical Nanostructures Laboratory, Columbia University, New York, New York 10027, USA*

[3]*OEwaves Inc., 465 N. Halstead Str., Pasadena, California 91107, USA*

[4]*Department of Physics, Columbia University, New York, New York 10027, USA*

**Corresponding author: cheewei.wong@ucla.edu*

Received February 17, 2015; revised May 1, 2015; accepted May 3, 2015;
posted May 5, 2015 (Doc. ID 234504); published May 28, 2015

We report on a study of a 698 nm extended cavity semiconductor laser with intracavity narrowband optical feedback from a whispering gallery mode resonator. This laser comprises an ultrahigh-Q ($>10^{10}$) resonator supporting stimulated Rayleigh scattering, a diffraction grating wavelength preselector, and a reflective semiconductor amplifier. Single longitudinal mode lasing is characterized with sub-kilohertz linewidth and a 9 nm coarse tuning range. The laser has a potential application for integration with the $^1S_0 - {}^3P_0$ strontium transition to create compact precision atomic clocks. © 2015 Optical Society of America

OCIS codes: (140.5960) Semiconductor lasers; (140.3518) Lasers, frequency modulated; (140.3600) Lasers, tunable; (140.4780) Optical resonators; (140.3425) Laser stabilization; (300.6260) Spectroscopy, diode lasers.
http://dx.doi.org/10.1364/OL.40.002596

Optical atomic clocks have the best known timing precision [1–7], serving as key timekeeping elements. This is possible because of the remarkable stability and narrow linewidth of optical transitions in ultracold atoms along with ultrastable narrow linewidth lasers used to interrogate and drive these transitions without inducing frequency shifts. Diode lasers are attractive here not only because of their compact nature but also their multiwavelength availability and tunability. The relatively high-frequency noise of these lasers is usually improved with an extended cavity or with a Bragg grating feedback frequency stabilization, resulting in linewidths of the order of tens of kilohertz (kHz) in either the Littman or Littrow configurations [8–13]. Further linewidth reduction can be achieved by locking the laser diode to an external high quality factor (Q) reference cavity. Active locking, like Pound–Drever–Hall (PDH) locking, is the conventional technique to reference the laser to the cavity resonances but an extra optical electronic feedback circuit is needed [14], which adds complexity and size to the system. An alternative technique is through passive self-injection locking of a free-running distributed feedback (DFB) or a Fabry–Perot (FP) laser diode by means of a high-Q resonator [15–19]. This technique is especially promising with monolithic whispering gallery mode (WGM) microresonators [20–22] due to their ultrahigh Q and the resonant Rayleigh backscattering, which occurs at the cavity resonant mode due to micro-inhomogeneities of the resonator [23,24]. Self-injection locking by means of this scattering, although still an external locking method outside the laser cavity, can result in a significant reduction of the laser phase noise in a broad frequency range [25–27], and atomic transition spectroscopy has been demonstrated with this method [28].

Ultrahigh-Q optical cavities usually have large spectral densities of optical states. A single resonant frequency mode within the semiconductor gain bandwidth is optimal for optical feedback in the self-injection-locking configuration, since multimode lasing and mode competition can occur if several modes produce equal optical feedback within the gain bandwidth. This problem exacerbates if the laser has an internal tendency of multimode operation like the FP lasers [18,19]. That is why only single-mode DFB lasers characterized with comparably high internal Q's are suitable for stable injection locking using multimode optical cavities.

DFB semiconductor laser chips, however, are unavailable at all desirable wavelengths corresponding to particular atomic optical transitions. Semiconductor optical amplifiers (SOA), on the other hand, are available in a much broader wavelength range. These SOAs, integrated with microresonators, can potentially form a modified extended cavity diode laser (ECDL) with ultra narrowband feedback, and unique and broadly tunable properties to match atomic clock transitions.

Here we report the first experimental demonstration, to our knowledge, of a single longitudinal mode ECDL with an integrated intracavity ultrahigh-Q WGM resonator. Our demonstration is at the 698 nm wavelength, relevant for strontium (Sr) optical clock transitions. Optical feedback responsible for the lasing occurs due to the resonant Rayleigh scattering inside the WGM resonator and, thus, the laser frequency is automatically locked to the WGM. A diffraction grating operates as a bandpass filter for selecting the proper WGM. The laser has a broad tuning range up to 9 nm limited by the gain bandwidth of the SOA chip. Continuous tuning is achieved by changing the grating angle along with the resonator temperature. Beating the emission of the ECDL with a ~100 Hz reference laser, we observed kHz-level linewidths. The resonant feedback efficiency is limited by power depletion through nonlinear processes of the ultrahigh-Q WGM resonator. This effect is not detrimental since optical clocks do not require high power and can be reduced by redesigning the WGM resonator with a larger mode and interrupted phase matching.

In our measurements, the WGM resonator is made from a magnesium fluoride (MgF_2) crystal with fine polishing [29]. The resonator has a toroidal shape, 7 mm in diameter and 0.1 mm in thickness, and is sealed

in a robust evanescent field-coupling package. The air gap between a coupling prism and the surface of the resonator is set with nanometer accuracy to achieve critical coupling at 698 nm. Rayleigh back-scattering is optimized at this condition, offering strong enough optical feedback to achieve lasing.

To measure the resonator Q, we built a conventional Littman–Metcalf ECDL utilizing a 698 nm reflective SOA chip (Sacher Lasertechnik Group). The setup schematic is shown in Fig. 1(a). Approximately 50% of light is reflected from the grating and used as the laser output, and 15% is fed back to the diode. The SOA had 3 dB gain bandwidth of 8 nm and is high-reflection coated on the back facet and antireflection coated on the front, to simplify optical feedback from an aligned diffraction grating. The laser beam is directed through an optical isolator and coupled to the WGM resonator. At this stage the ECDL does not involve WGM resonator feedback, serving only to probe the cold resonator modes. By changing the injection current of the gain chip, the laser frequency is scanned through WGM resonances for the linewidth measurements. Light from the resonator is sent to a slow photodiode and the photocurrent is analyzed with an oscilloscope. As shown in Fig. 2, a number of resonance dips are observed in this scan because of the high mode density of the WGM resonator.

We observe Q's of the order of a billion for most of the lower order modes. However, two particular mode families demonstrated exceptionally narrow linewidths of 45 and 30 kHz, respectively, which correspond to Q of 9.5×10^9 and 1.4×10^{10}. The transmission spectra of the modes are shown in the insets of Fig. 2. The spectrum is noisy since the ECDL linewidth was less than 50 kHz, comparable with the measured WGM linewidths.

We then achieve a self-injection-locked ECDL with the resonator by removing the isolator, while maintaining the Littman–Metcalf configuration in Fig. 1(a). The transmission swept over 10 GHz is shown in Fig. 3. Resonant-stimulated Rayleigh scattering in the WGM resonator feedbacks to the SOA to self-injection lock the laser frequency. The actual lasing frequency starts to follow the WGM frequency. Consequently, the frequency of the self-injection-locked laser does not change when the laser is attempted to be tuned by the injection current. The dynamic range of this locking is determined by the ratio of the Q's as well as the optical feedback efficiency. As shown in the inset of Fig. 3, the laser frequency is pulled over 80 MHz away from its original lasing frequency when locked to the high-Q WGM. While locking up to a dynamic range of 300 MHz is observed, it is not stable because of the phase-sensitive interference from the multiple optical resonant loops (such as an ECDL, the WGM resonator, and the ECDL–WGM coupling).

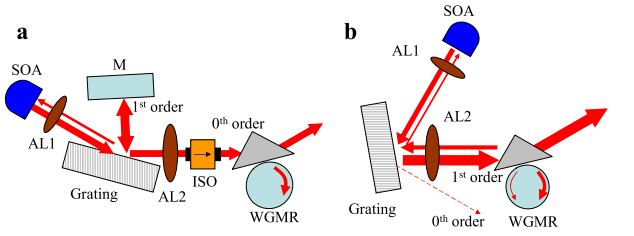

Fig. 1. (a) Cold cavity measurement schematic with the Littman–Metcalf ECDL configuration. (b) Schematic of the WGM-ECDL. AL1 and AL2, aspheric lenses, WGMR, whispering gallery mode resonator; ISO, isolator; M, mirror.

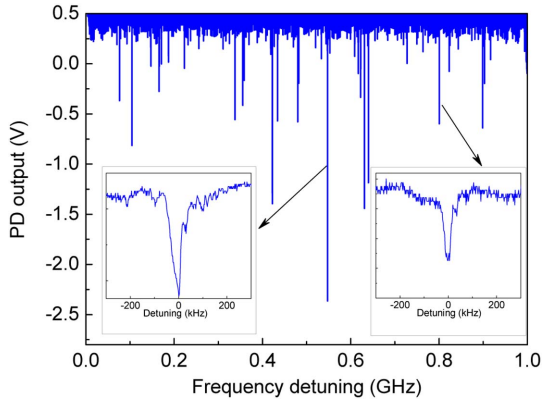

Fig. 2. Transmission spectra of the 698 nm WGMs package. Inset: zoom-in of the cold cavity resonances with measured linewidths of 30 and 45 kHz, respectively, corresponding to visible wavelength Q of 14.3 and 9.5 billion. It is worth noting that the spectrum density can be substantially reduced by changing the shape of the resonator.

To achieve stable lasing from SOA and utilize the ultra narrowband feedback from the WGM resonator, we build an ECDL with an integrated WGM resonator (WGM-ECDL), as shown in Fig. 1(b) in comparison with the conventional Littman–Metcalf configuration. The 698 nm SOA serves as the gain medium and is temperature stabilized with the resonator and the laser frame, down to the milliKelvin level in our measurements. The SOA broadband emission is collimated by an aspheric lens AL1 and directed onto the ruled diffraction grating. The grating transfers approximately 80% of the input radiation to the first-order beam, subsequently directed into the WGM resonator. The grating spectral

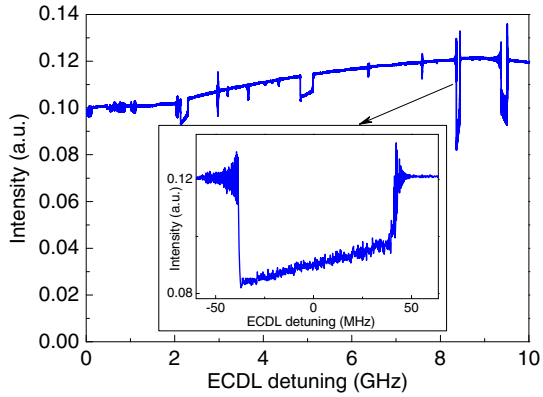

Fig. 3. Observations of self-injection locking by sweeping frequency of the Littman–Metcalf ECDL [see Fig. 1(a)] with the isolator removed. The laser frequency is pulled away from the sweep when the laser locks to a WGM, illustrated by the sharp dips in transmission during laser detuning. Zoom-in of one resonance dip shows over 80 MHz cavity pulling when the laser is injection-locked. Broader lower-contrast regions of self-injection locking are also observed. Those regions originate from higher order cavity modes with weaker mode matching with the drive laser.

resolution is measured to be around 200 pm full-width at half-maximum. This filtering is important to achieve single longitudinal mode lasing, considering the high mode density of the WGM resonator. A second aspheric lens AL2 focuses the diffracted beam to the packaged coupling prism to achieve mode matching with a selected WGM. The numerical aperture matching between the SOA and WGM is realized by optimizing the ratio between AL1 and AL2.

The resonator acts as a narrowband reflector in the Littman–Metcalf configuration. Its Rayleigh backscattering satisfies the resonance condition and results in at least 5% feedback of the scattered light, sufficiently strong to result in lasing of the system. The backscattered spectral bandwidth into the SOA is defined by the linewidth of the selected ultrahigh-Q WGM. Figure 4 shows the tuning of output wavelength from 690.3 to 699.3 nm by changing the grating angle (measured by an Advantest Q8384 optical spectrum analyzer). The 9 nm tuning range agrees well with the approximately 8 nm gain bandwidth of the SOA. About 2 mW output can be measured. In our approach, no additional feedback mechanisms other than the Rayleigh backscattering is required. This prevents feedback competition and allows better stability, where our laser configuration operates much more steadily without mode-hopping compared with the prior self-injection-locking Littman–Metcalf ECDL.

Furthermore, we note that while a bare SOA did not produce coherent light, it shows a clear current threshold for amplified spontaneous emission (ASE) at 44 mA. The actual lasing threshold was lowered to 32 mA by optimizing the coupling to the selected WGM. Above the lasing threshold, over 10 dB ASE power suppression is measured throughout the 9 nm tuning range.

We next examine the short-term stability of the WGM-ECDL by beating with a reference laser at a 50:50 fiber coupler, while both lasers are tuned to 698 nm. The reference laser is locked to a temperature-stabilized and mechanically isolated bulk Fabry–Perot cavity using the Pound–Drever–Hall approach, with a calibrated instantaneous linewidth of the order of 100 Hz. The beat signal is detected by a fast photodiode and processed with a RF spectrum analyzer with 500 Hz resolution. The result is shown in the inset of Fig. 4. The RF beat signal is fitted with a 1 kHz linewidth, indicating 1-kHz level instantaneous linewidth of the WGM-ECDL. The reference laser does not contribute significantly to the RF linewidth since it has much smaller frequency noise. Better temperature stabilization and mechanical isolation of the resonator and ECDL housing can further improve the ECDL performance at longer time scales.

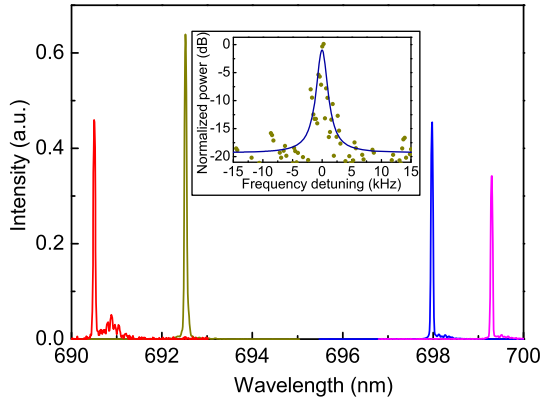

Fig. 4. Measured spectra at different lasing wavelengths through tuning of the cavity and the feedback roundtrip with the injection current. The inset illustrates the ECDL linewidth measured by beating the lasing emission with a reference 100 Hz bulk FP laser on a fast photodiode. The Lorentzian fit (blue solid line) shows the 1 kHz beat linewidth.

The short-term fluctuations of the laser frequency can be improved by increasing optical feedback from the resonator, which is limited here by nonlinear processes at high power levels. Intracavity hyperparametric oscillation can be observed in the WGM-ECDL with a threshold injection current of about 60 mA, because of the very high Q and small mode volume of the resonator. Broadband parametric light generation can be observed depending on the phase matching, determined by the selection of the resonator mode in which the laser operates. The parametric process results in decreasing of the intracavity power and reduction of the feedback to the SOA. It also leads to the slow WGM resonance drift on the MHz level via thermal refraction coupling. To achieve better performance of the WGM-ECDL, we can change the geometric design of resonator. Larger WGM mode size is preferred and the phase match can be interrupted for hyperparametric scattering. Another opportunity is related to the reduction of the Q-factor at parametric wavelengths using a special coating. By suppressing the nonlinear effects in the WGM resonator, thermal-noise-limited performance may be expected [22,30] and long-term stability can be also improved.

While the observed nonlinear process is undesirable for the laser operation, it can be considered as a clear indication that our laser produces highly coherent radiation and may be used for spectral span extension in the future. Figure 5 shows the hyperparametric spectrum captured by a CCD spectrometer. Two pairs of signal and idler modes can be observed, with a maximum frequency separation of 137.2 THz. The inset of Fig. 5 shows a picture of our WGM resonator when hyperparametric oscillation occurs, where the WGM resonator glows red, in our packaged WGM-ECDL lasing architecture.

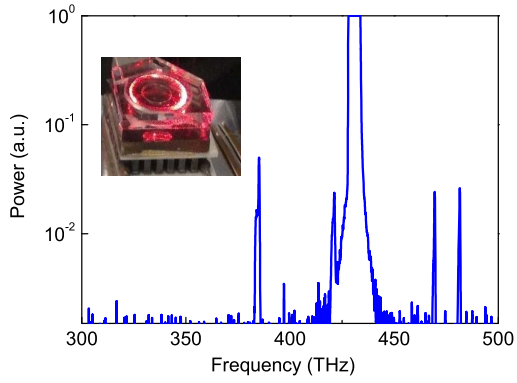

Fig. 5. Nonlinear frequency conversion observed in the WGM resonator when the power of the light confined in the selected WGM exceeds a certain threshold. The inset shows a glowing WGM resonator in a thermally stabilized package.

A similar effect is also observed in a self-injection-locking scheme and the details can be found in Ref. [31].

In conclusion, we have developed a narrow linewidth 698 nm laser using a semiconductor reflective amplifier and an ultrahigh-Q MgF_2 WGM resonator. No external feedback loop is involved in this approach. With the WGM resonator embedded within the laser cavity, stimulated Rayleigh backscattering is utilized as the lasing feedback to achieve a kHz short-term laser linewidth. A 1 kHz beat linewidth is achieved when referenced against a bulk-cavity-stabilized 698 nm laser. A tunable range of up to 9 nm is achieved, bounded by the gain chip bandwidth. The demonstrated compact laser is suitable for the $^1S_0 - {}^3P_0$ transition in Sr atoms, and our WGM-ECDL architecture is applicable across a broad range of wavelengths. It is possible to develop an optical frequency standard with high stability and in a compact simple package by locking this ECDL to atomic transitions.

The authors acknowledge assistance from James F. McMillan, Benjamin W. Aguilar, Noam Goldberg, Dov Fields, and Gael Reinaudi. Defense Sciences Office of the Defense Advanced Research Projects Agency (W911QX-13-C-0141); Air Force Office of Scientific Research (FA9453-14-M-0090) partially funded this work. M. M. thanks NSF IGGRT DGG-2069240.

References

1. S. A. Diddams, T. Udem, J. C. Bergquist, E. A. Curtis, R. E. Drullinger, L. Hollberg, W. M. Itano, W. D. Lee, C. W. Oates, K. R. Vogel, and D. J. Wineland, Science **293**, 825 (2001).
2. T. Udem, R. Holzwarth, and T. W. Hänsch, Nature **416**, 233 (2002).
3. L.-S. Ma, Z. Bi, A. Bartels, L. Robertsson, M. Zucco, R. S. Windeler, G. Wilpers, C. Oates, L. Hollberg, and S. A. Diddams, Science **303**, 1843 (2004).
4. S. A. Diddams, J. C. Bergquist, S. R. Jefferts, and C. W. Oates, Science **306**, 1318 (2004).
5. A. Derevianko and H. Katori, Rev. Mod. Phys. **83**, 331 (2011).
6. N. Hinkley, J. A. Sherman, N. B. Phillips, M. Schioppo, N. D. Lemke, K. Beloy, M. Pizzocaro, C. W. Oates, and A. D. Ludlow, Science **341**, 1215 (2013).
7. B. J. Bloom, T. L. Nicholson, J. R. Williams, S. L. Campbell, M. Bishof, X. Zhang, W. Zhang, S. L. Bromley, and J. Ye, Nature **506**, 71 (2014).
8. M. G. Littman and H. J. Metcalf, Appl. Opt. **17**, 2224 (1978).
9. K. Liu and M. G. Littman, Opt. Lett. **6**, 117 (1981).
10. K. C. Harvey and C. J. Myatt, Opt. Lett. **16**, 910 (1991).
11. S. Lecomte, E. Fretel, G. Mileti, and P. Thomann, Appl. Opt. **39**, 1426 (2000).
12. L. Ricci, M. Weidemuller, T. Esslinger, A. Hemmerich, C. Zimmermann, V. Vuletic, W. Konig, and T. W. Hänsch, Opt. Commun. **117**, 541 (1995).
13. C. J. Hawthorn, K. P. Weber, and R. E. Scholtena, Rev. Sci. Instrum. **72**, 4477 (2001).
14. J. Alnis, A. Schliesser, C. Y. Wang, J. Hofer, T. J. Kippenberg, and T. W. Hänsch, Phys. Rev. A **84**, 011804(R) (2011).
15. B. Dahmani, L. Hollberg, and R. Drullinger, Opt. Lett. **12**, 876 (1987).
16. L. Hollberg and M. Ohtsu, Appl. Phys. Lett. **53**, 944 (1988).
17. A. Hemmerich, C. Zimmermann, and T. W. Hänsch, Appl. Opt. **33**, 988 (1994).
18. Y. Zhao, Y. Li, Q. Wang, F. Meng, Y. Lin, S. Wang, B. Lin, S. Cao, J. Cao, Z. Fang, T. Li, and E. Zang, IEEE Photon. Technol. Lett. **24**, 1795 (2012).
19. Y. Zhao, Y. Peng, T. Yang, Y. Li, Q. Wang, F. Meng, J. Cao, Z. Fang, T. Li, and E. Zang, Opt. Lett. **36**, 34 (2011).
20. V. V. Vassiliev, V. L. Velichansky, V. S. Ilchenko, M. L. Gorodetsky, L. Hollberg, and A. V. Yarovitsky, Opt. Commun. **158**, 305 (1998).
21. V. V. Vassiliev, S. M. Ilina, and V. L. Velichansky, Appl. Phys. B **76**, 521 (2003).
22. W. Liang, V. S. Ilchenko, A. A. Savchenkov, A. B. Matsko, D. Seidel, and L. Maleki, Opt. Lett. **35**, 2822 (2010).
23. D. S. Weiss, V. Sandoghdar, J. Hare, V. Lefevre-Seguin, J.-M. Raimond, and S. Haroche, Opt. Lett. **20**, 1835 (1995).
24. M. L. Gorodetsky, A. D. Pryamikov, and V. S. Ilchenko, J. Opt. Soc. Am. B **17**, 1051 (2000).
25. H. Li and N. B. Abraham, Appl. Phys. Lett. **53**, 2257 (1988).
26. H. Li and N. B. Abraham, IEEE J. Quantum Electron. **25**, 1782 (1989).
27. P. Laurent, A. Clairon, and C. Breant, IEEE J. Quantum Electron. **25**, 1131 (1989).
28. A. A. Savchenkov, D. Eliyahu, W. Liang, V. S. Ilchenko, J. Byrd, A. B. Matsko, D. Seidel, and L. Maleki, Opt. Lett. **38**, 2636 (2013).
29. I. S. Grudinin, V. S. Ilchenko, and L. Maleki, Phys. Rev. A **74**, 063806 (2006).
30. A. A. Savchenkov, A. B. Matsko, V. S. Ilchenko, N. Yu, and L. Maleki, J. Opt. Soc. Am. B **24**, 2988 (2007).
31. W. Liang, A. A. Savchenkov, Z. D. Xie, J. F. McMillan, J. Burkhart, V. S. Ilchenko, C. W. Wong, A. B. Matsko, and L. Maleki, Optica **2**, 40 (2015).